Active Calibration Target for Bistatic Radar Cross-Section Measurements

M. Pienaar[1], J. W. Odendaal[1], J. Joubert[1], J. E. Cilliers[2], and J. C. Smit[2]

[1]Centre for Electromagnetism, Department of Electrical, Electronic and Computer Engineering, University of Pretoria, Pretoria 0002, South Africa.

[2]Defence Peace Safety and Security, Council for Scientific and Industrial Research, Pretoria 0002, South Africa.

Corresponding author: Johann Odendaal (wimpie@up.ac.za)

Key Points:

- An active calibration target as reference target for bistatic RCS measurements.
- The target is simple to manufacture, lightweight and compact for airborne deployment via a remote controlled drone.

Abstract

Either passive calibration targets are expensive and complex to manufacture or their bistatic RCS levels are significantly lower than the monostatic RCS levels of targets such as spheres, dihedral- and trihedral corner reflectors. In this paper the performance of an active calibration target with relative high bistatic RCS values is illustrated as a reference target for bistatic RCS measurements. The reference target is simple to manufacture, operates over a wide frequency range and can be configured to calibrate all four polarizations (VV, HH, HV and VH). Bistatic RCS measurements of canonical targets, performed in a controlled environment, are calibrated with the reference target and the results are compared to simulated results using FEKO.

1 Introduction

Bistatic radars appeared simultaneously in the United Kingdom, France, Russia, Italy, Japan and the United States [*Glaser,* 1986], [*Glaser,* 1989]. It was only around the early 1950s that the interest in bistatic radars for aircraft detection increased [*Skolnik,* 2008]. The measurement of bistatic radar cross section (RCS) has the potential to improve characterization and identification of stealth targets since many targets are shaped such that the reflected energy is directed away from the radar transmitter (monostatic scattering) [*Griffiths,* 2013], [*Burkholder et al.,* 2003], [*Eigel* et al., 2000]. This increases target information in the bistatic scenario [*Kahny et al.,*1992], by adding an additional dimension [*Eigel* et al., 2000]. Target classification requires full characteristic information regarding the target, this is achieved by utilizing wideband full bistatic RCS signatures [*Monzon,* 2003]. The transmitter and receiver for a bistatic radars are physically separated by a considerable distance [*Kesheng,* 2003], [*Skolnik,* 2008] in contrast to monostatic radar where the transmitter and receiver are located at the same position [*Glaser,* 1989]. The advantage of bistatic radar is that its receiving system is completely passive which makes it covert and undetectable by enemy systems [*Griffiths,* 2013]. Another application of bistatic radars investigated in the 1970s and 1980s was counters to anti-radiation missiles and jammers [*Skolnik,* 2008]. The problem with bistatic radar systems is that the transmitter and receiver must be synchronized, which can prove difficult to achieve [*Kesheng,* 2003]. Synchronization is one of the most important challenges of bistatic radars [*Haung et al.,* 2006]. Solving this problem has become less difficult due to the improvement of Global Navigation Satellite System (GNSS) based synchronization systems [*Griffiths,* 2013].

Accurate calibrated bistatic measurements are important since bistatic radar cross section can improve characterization and identification of military targets. Calibration of monostatic radar systems has been studied extensively and is well understood, but for bistatic radar systems the calibration problem is significantly more complex and little information is available describing the calibration of these systems [*Bradley et al.,* 2001], [*Daout et al.,* 1996]. Fully polarimetric bistatic radar systems are more complex compared to single-polarization bistatic systems or monostatic systems. These complexities significantly affect the requirements for calibration. A major component which adds to the complexity is the polarization performance of the calibration target [*Bradley et al.,* 2005]. A fully polarimetric system needs calibration in vertical transmit - vertical receive (VV) polarization; horizontal transmit - horizontal receive (HH) polarization; vertical transmit - horizontal receive (VH) polarization and horizontal transmit - vertical receive (HV) polarization. Important aspects to consider when selecting a calibration target are: the bistatic scattering pattern across the angular region of interest; the intensity of scattering across the angular region of interest; and the availability of different

polarization configurations [*Bradley et al.*, 2005]. According to [*Bradley et al.*, 2001] there are no known passive calibration targets with bistatic RCS levels equivalent to the monostatic levels of targets such as dihedral- and trihedral corner reflectors. Dihedral- and trihedral corner reflectors are however not suitable for bistatic radar calibration [*Bradley et al.*, 2005]. In 2003, a passive cross-polarization calibration target was designed for bistatic RCS calibration [*Monzon*, 2003]. Although this device performed well over a wide frequency range, it is a very complex structure to design and manufacture.

In this paper the performance of an active calibration target that is simple to manufacture, operates over a wide frequency range and can be configured to calibrate all four polarization configurations, VV-, HH-, VH- and HV-polarization, is illustrated as a reference target for bistatic RCS measurements. The performance of the active calibration target was demonstrated by conducting bistatic RCS measurements in a controlled environment, viz. the compact range at the University of Pretoria in South Africa [*Janse van Rensburg et al.*, 1992]. Bistatic RCS measurements of canonical shapes were obtained in the compact range at bistatic angles of $\beta = 45°$ and $\beta = 90°$ and the Multilevel Fast Multipole Method (MLFMM) was used in FEKO simulations to validate the accuracy of the bistatic RCS measurements.

2 Theoretical background

Calibration is an interpretation of the raw data measured for the device under test (DUT) based on the relationship between the calibration target measurements and its true/theoretical RCS values [*Bradley et al.*, 2005]. The standard calibration process involves measuring the complex back scattered field from the calibration (reference) target with known absolute RCS values [*Knott et al.*, 2004].

The calibrated RCS of the DUT is expressed as [*Bradley et al.*, 2005]

$$RCS_{DUT} = \left(\frac{E_{DUT} - E_{DUT,back}}{E_{Ref} - E_{Ref,back}} \right) \sigma_{Calib} \qquad (1)$$

where RCS_{DUT} is the calibrated scattering of the target. E_{DUT} is the complex value of the bistatic scattered field from the DUT, E_{Ref} is the complex value of the bistatic scattered field from the calibration target. $E_{DUT,back}$ is the complex value of the background measurement with no target in the compact range and $E_{Ref,back}$ is the complex value of the background for the reference target setup, if different from the setup of the DUT. σ_{Calib} is the theoretical or measured RCS response of the calibration target and is known a priori. The RCS response of the active calibration target was measured in the compact range using a monostatic setup, calibrated with a sphere as reference target.

Selecting a calibration target is critical to ensure accurate RCS data with a high degree of repeatability. Usually a conducting sphere is used as a reference target for monostatic measurements in the compact range because the monostatic RCS of a sphere is independent of incidence angle. The bistatic RCS setup of a 6 inch perfect electric conductor (PEC) sphere simulated in FEKO is shown in Fig. 1, for incident field at $\theta = \phi = 0°$ and bistatic angle $0° \leq \beta \leq$

360° in the θ direction. A frequency sweep was performed from 2 GHz – 8 GHz covering the frequency range of the active calibration target. The simulated results are shown in Fig. 2

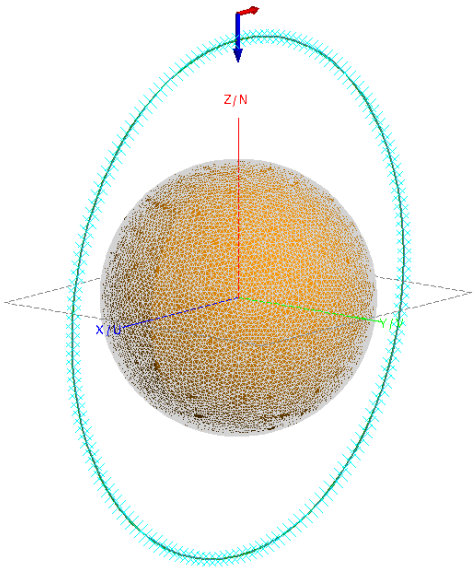

Figure 1. Bistatic RCS setup of a PEC sphere in FEKO..

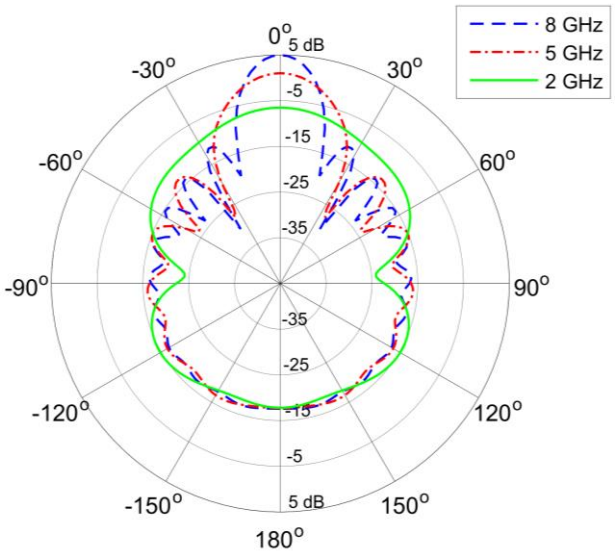

Figure 2. Bistatic RCS of a conducting sphere (diameter 156 mm), with incident field at 0°, for 2GHz, 5GHz and 8GHz.

The bistatic RCS of a conducting sphere has nulls at large bistatic angles which make it unsuitable as a bistatic calibration target. At 2 GHz nulls occur in the bistatic response at angles close to -90° and 90°. As the frequency increases to 5 GHz and 8 GHz the bistatic aspect angle without nulls decreases significantly, rendering the sphere unusable as reference target for large bistatic angles. Another disadvantage of using a sphere is that it can only be used to calibrate VV- and HH-polarization configurations, since its cross-polarization levels are negligible [*Sarabandi et al.*, 1990]. These attributes of a sphere eliminate it as a versatile calibration target for bistatic calibration. Other possible calibration targets which have significant cross-

polarization levels include dihedral corner reflectors but these structures are sensitive to alignment inaccuracies which decrease measurement accuracy [*Bradley et al.,* 2005], [*Sarabandi et al.,* 1990]. [*Bradley et al.,* 2005] did a study to evaluate the suitability of various shapes as bistatic calibration targets. Seven shapes were investigated which included a PEC sphere, long cylinder, short cylinder, dihedral corner reflector, circular disk, wire mesh and a trihedral corner reflector. It was found that trihedral corner reflectors are not suitable for bistatic calibration and dihedrals are more useful for monostatic calibration purposes. Flat plates, cylinders and disks were found to be good calibration objects at small bistatic angles. The wire mesh (not considered a canonical object) proved to be a good polarimetric calibration target at small bistatic angles. An active calibration target seemed to alleviate all the problems experienced with the shapes investigated in [*Bradley et al.,* 2005]. An active calibration target has high RCS return over a large frequency range and can easily be configured for different bistatic angles and for significant cross-polarization levels to calibrate VH and HV.

3 Measurement setup and RCS results

The standard configuration of the compact range for monostatic RCS measurements uses a parabolic reflector for transmit as well as receive. In order to allow for bistatic RCS measurements in the anechoic chamber the parabolic reflector was used for transmit to create a plane wave illumination. The incident field was thus at an azimuth angle of 0°. A wideband double ridged guide horn antenna was mounted to the side of the chamber for receive, as shown in the top-view schematic in Fig 3. and in the picture in Fig. 4.

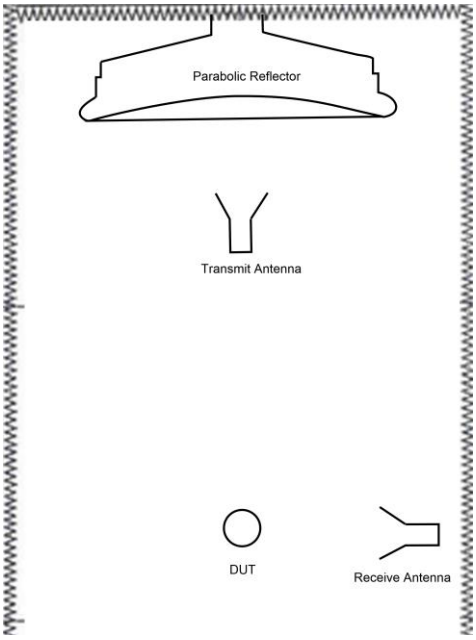

Figure 3. Top-view schematic of the compact range setup for bistatic measurement scenario, $\beta = 90^0$

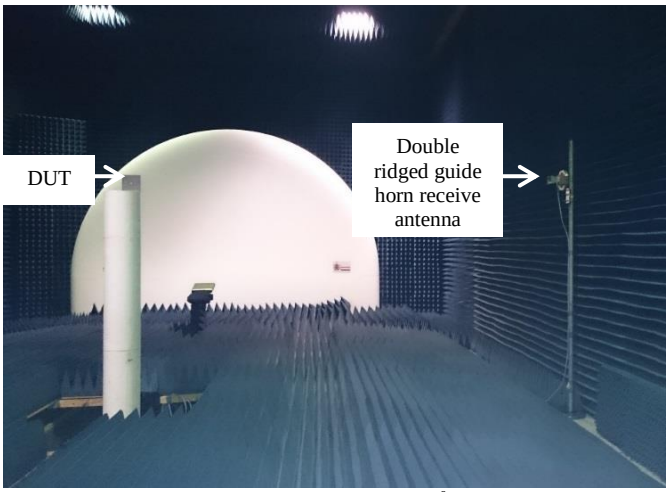

Figure 4. Bistatic RCS measurement setup ($\beta = 90^0$) in the compact range for a dihedral corner reflector as the DUT.

Bistatic measurements were performed for two bistatic angle setups viz. β = 45° and β = 90°. The receive antenna was placed at angles of +45° and +90° in azimuth relative to the incident field, respectively. The distance between the DUT mounted on a polystyrene column and the receive antenna was 4 m for a bistatic angle of β = 90° and 5.7 m for β = 45° to comply with the far field criteria, [*Balanis,* 2009]

$$r \geq 2\left(\frac{D^2}{\lambda}\right) \qquad (2)$$

where r is the distance between target and receive antenna, D is the largest dimension of the DUT and λ is the wavelength for highest frequency. This limits the maximum dimension of the DUT to 300 mm at 6 GHz. The devices under test were a flat metal plate (150 mm x 150 mm) and a metal dihedral corner reflector (150 mm x 150 mm x 150 mm).

The active calibration reference target shown in Fig. 5 with top view schematics in Fig. 6, was measured with the same bistatic angles **(**β = 45° and β = 90°**)** as the DUTs from 2.5 GHz to 6 GHz. The active calibration target consists of two wideband Vivaldi antennas, one for transmit and one for receive; an optional attenuator; an isolator and an amplifier. Vivaldi antennas were implemented since they can be designed to have large frequency bands, broad beamwidths and low cross-polarization levels [*Vu et al.,* 2009]. The optional attenuator can be used to control the RCS response of the target. The amplifier increases the effective RCS of the calibration target. The isolator was implemented to protect the amplifier from feedback between the transmit and receive antennas. The theoretical RCS of the active calibration target is [*Ahne et al.,* 1993].

$$\sigma_{eff} = G_{loop}\frac{G_r G_t \lambda^2}{4\pi} \qquad (3)$$

where G_{loop} is the effective gain of the loop elements (RF amplifier, isolator, attenuator and connecting cables); G_t and G_r are the gains of the transmit and receive Vivaldi antennas, respectively and λ is the radar wavelength.

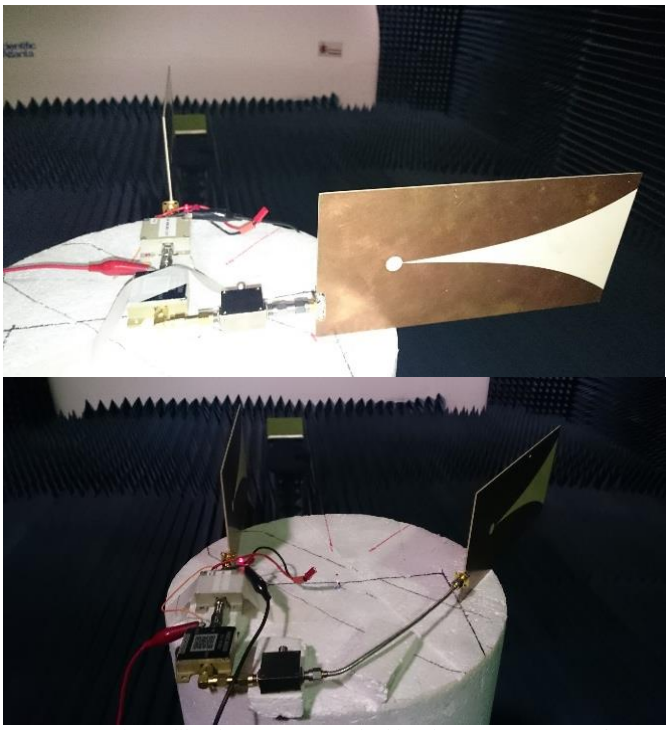

Figure 5. Active calibration target setup for bistatic measurements at β = 90° (top) and at β = 45° (bottom), VV-polarization.

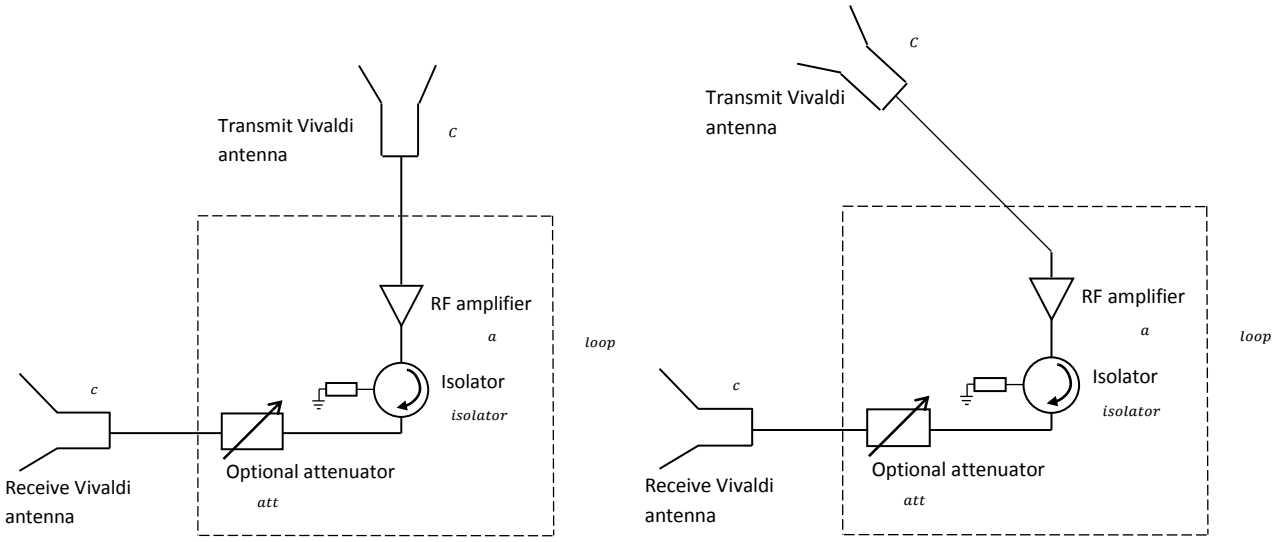

(a) **(b)**

Figure 6. Active calibration target setup for bistatic measurements (a) β = 90° and (b) β = 45°.

The measurement setup to characterize the RCS response of the active calibration target for VH-polarization is shown in Fig. 7. The measured frequency response of the active calibration target at VV-, HH- and VH-polarization is shown in Fig. 8. The response for horizontal-vertical (HV) polarization is the same as for VH-polarization.

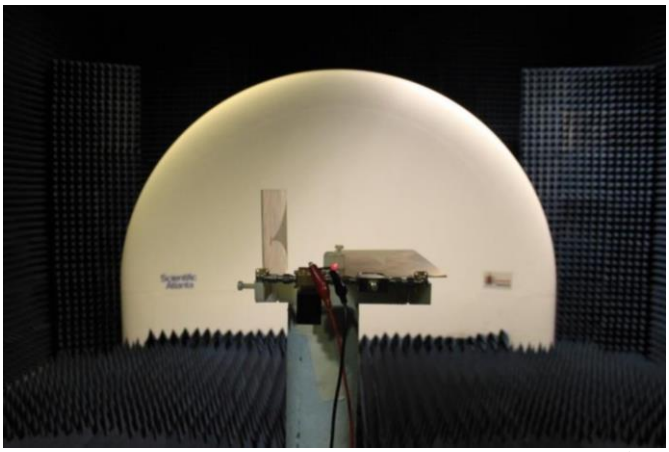

Figure 7. The active calibration target measured in the compact range for VH-polarization.

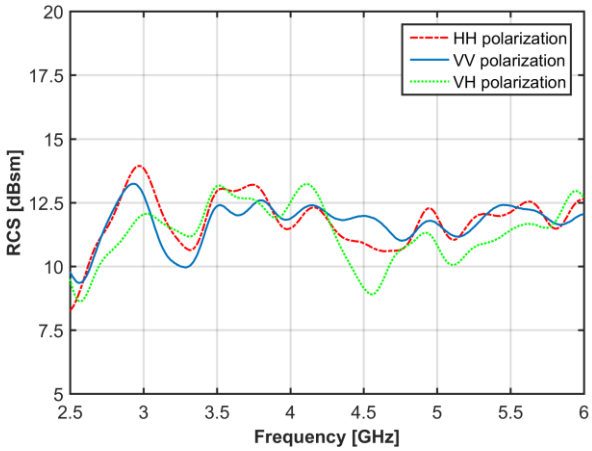

Figure 8. Frequency response of the active calibration target for VV-, HH- and VH-polarization.

The reference measurement with the active bistatic calibration target is performed as a frequency sweep at a discrete bistatic angle, with the receive antenna pointing in the direction of the radar transmitter and the transmit antenna pointing to the radar receiver. The wide beamwidths of the Vivaldi antennas reduce sensitivity to possible alignment errors. The principle plane radiation patterns for the Vivaldi antennas at 3.5 GHz are shown in Fig. 9. The 1 dB E-plane beamwidth is 21.3° and the 1 dB H-plane beamwidth is 40°.

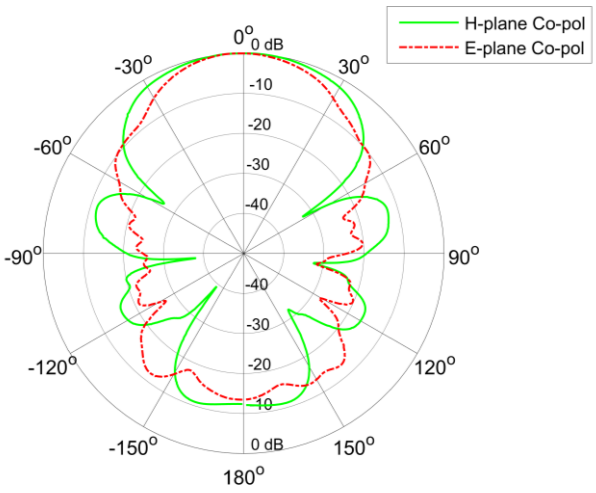

Figure 9. . E-plane co-polarization radiation pattern and H-plane co-polarization radiation pattern at 3.5 GHz.

The measurement setup for bistatic RCS (VV-polarization) of a flat conducting plate at a bistatic angle of $\beta = 90°$, is shown in Fig. 10. The plate was rotated from -10° to 120° relative to the incident field and calibrated with the active calibration target measured at the same bistatic angle in VV-polarization configuration.

The measured and simulated (using FEKO) bistatic RCS results of the flat metal plate at a bistatic angle of 90° are shown in Fig. 11. There is a good agreement between the bistatic RCS measurements and FEKO simulations. The bistatic RCS of the flat conducting plate has a peak at an aspect angle of 45°, between the transmitter at 0° and the receiver at 90°. The maximum difference between the measured and simulated RCS values in the main lobe is only 0.47 dB. The bistatic RCS (VV-polarization) of the same plate was measured in the compact range at a bistatic angle of $\beta = 45°$. The plate was rotated from -90° to 120° and it was calibrated with the

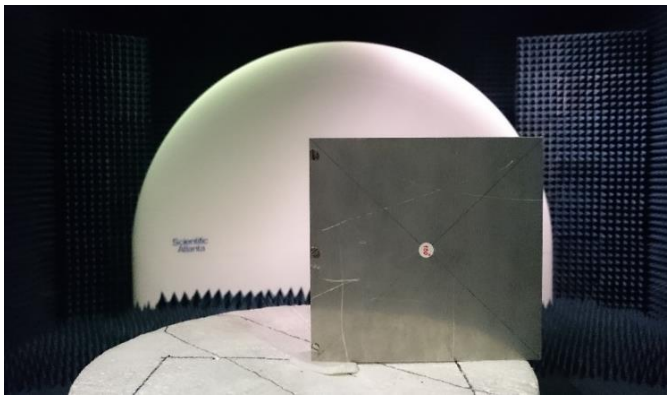

Figure 10. Flat plate setup on the pedestal in the compact range.

active calibration target measured at a bistatic angle of β = 45°. The measured and simulated data are shown in Fig. 12.

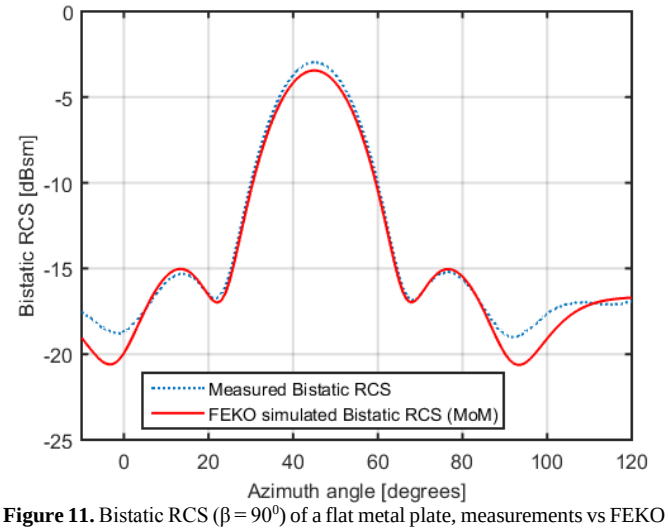

Figure 11. Bistatic RCS ($\beta = 90^0$) of a flat metal plate, measurements vs FEKO simulations; VV-polarization.

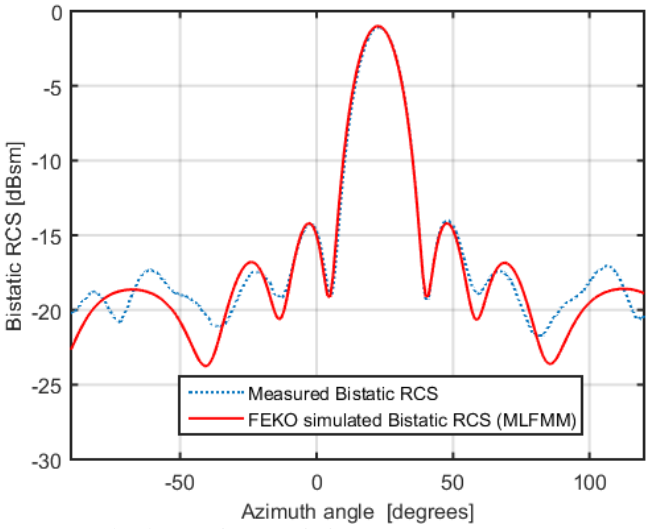

Figure 12. Bistatic RCS (β = 45°) of a flat metal plate, measurements vs FEKO simulations; VV-polarization.

There is a good agreement between the bistatic RCS measurements and FEKO simulations - the two data sets follow the same trend. The peak (-1.08 dBsm) return for the flat metal plates is situated at 22.5°, which is halfway between the transmitter and receiver angles. The maximum difference between the measured and simulated data from -3° to 48° is 0.47 dB, and at angles further from the main lobe a maximum differences of 2.05 dB is noted. The

maximum difference between the simulated and measured data is approximately 3 dB at ± 63° from the main lobe.

The bistatic RCS (VV-polarization) of the dihedral corner reflector measured at a bistatic angle of β = 90° for azimuth rotation angles from -180° to 180° are shown in Fig. 13.

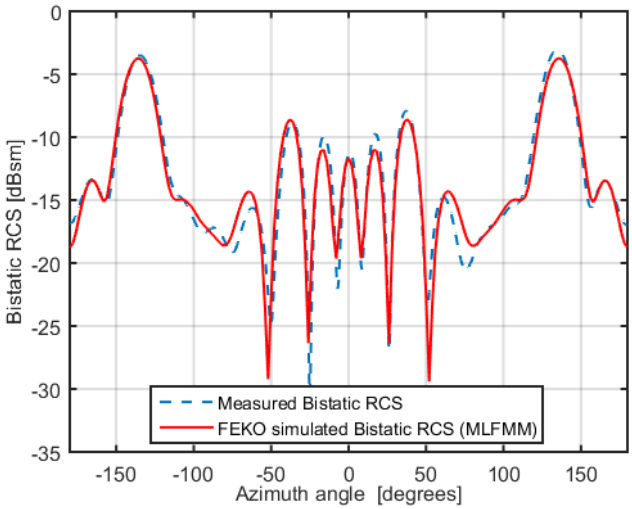

Figure 13. Bistatic RCS (β = 90°) of a dihedral corner reflector, measurements vs FEKO simulations; VV-polarization.

The measured and simulated data follow the same pattern with peaks at 135° and -135°, when the incident angle on the plate side of the dihedral was at 45°. The slight offset in angle can be due to a minor misalignment in the measurement setup. This measurement was repeated for

VV-polarization and β = 45°. The comparison of measured and simulated data is given in Fig. 14.

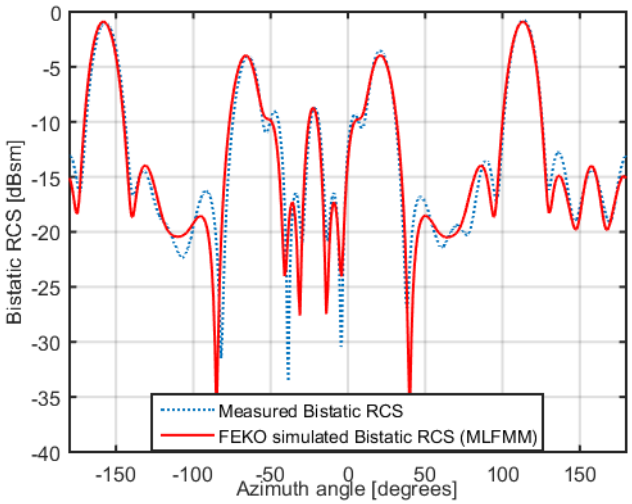

Figure 14. Bistatic RCS (β = 45°) of a dihedral corner reflector, measurements vs FEKO simulations; VV-polarization.

The measured and simulated data have the same form, with peaks at + 122.5° and -157.5°, when the incident angle on the outside of the dihedral is at 22.5° relative to the

transmitter. The values of the five main peaks for the measured and simulated data are almost identical.

The RCS of the conducting plate was measured over a frequency range from 2.5 GHz to 6 GHz for VV- and HH-polarization. The plate was positioned at an angle of 45° and the bistatic angle was β = 90°. The simulated versus measured results are shown in Fig. 15.

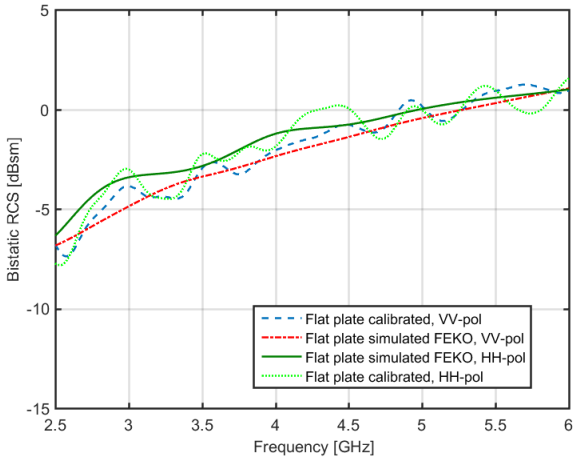

Figure 15. Flat metal plate frequency sweep β, = 90°, VV-polarization and HH-polarization, plate rotated at 45°.

There is a good agreement between the measured and simulated data over this broad frequency range. The maximum difference for VV-polarization between the measured and simulated data is 1.03 dB. The maximum difference for HH-polarization between the measured and simulated data is 1.88 dB.

4 Conclusions

Passive calibration targets are either expensive and complex to manufacture or their bistatic RCS levels are significantly lower than the monostatic RCS levels of targets such as spheres, dihedral- and trihedral corner reflectors. The complex shaped passive bistatic calibration target designed by Monzon is difficult to manufacture [*Monzon*, 2003]. The bistatic RCS amplitude of this calibration target can't easily be adjusted since it is a passive target. According to a study of bistatic calibration targets by [*Bradley*, 2005] a sphere needs to be physically large to produce an RCS high enough for calibration and dihedral and trihedral corner reflector can't be used as bistatic calibration targets for large bistatic angles. Spheres, disks and flat plates were considered good calibration targets at small bistatic angles. The wire mesh was also considered and although it is a good polarimetric calibration target, it only works at small bistatic angles. The RCS of the wire mesh was relatively small which will make calibration difficult. The active bistatic calibration target has the advantage of high (adjustable) bistatic RCS returns in all four polarization configurations. It can also be used to calibrate bistatic scenarios with small or large bistatic angles. The uncertainties associated with the calibration of ground to air bistatic radar systems as well as passive calibration targets have motivated the use of an active calibration target as a reference for bistatic RCS measurements. In this paper the

performance of an active calibration target that is simple to manufacture, operates over a wide frequency range and can be configured to calibrate all four polarizations (VV, HH, HV and VH) was demonstrated as a reference target for bistatic RCS measurements. This calibration target can be used to calibrate a large range of bistatic configuration setups which is a major advantage. The active calibration target used in this paper is lightweight and compact which enables deployment via a remote controlled drone as was demonstrated in [*Pienaar et al.,* 2015] for monostatic RCS measurements.

Acknowledgments and Data

The authors are grateful for the support received from Ernst Burger at Altair FEKO.

References

Ahne, J. J., Sarabandi, K., and F. T. Ulaby, (1993), Design and implementation of single antenna polarimetric active radar calibrators, International Symposium on Antenna and Propagation Society, United States of America.

Balanis, C. A., (2009) Antenna Theory: Analysis and Design, Wiley, United States of America.

Bradley, C. J., Collins, P. J., Temple, M. A., Terzuoli, A. J., Nesti, G., Fortuny, J., and G. D. Lewis, (2001), Issues in the calibration of bistatic RCS measurements, Eleventh International Conference on Antennas and Propagation, Manchester.

Bradley, C. J., Collins, P. J., Fortuny-Guasch, J., Hastriter, M. L., Nesti, G., Trezouli, A. J., and K. S. Wilson (2005), An investigation of bistatic calibration objects, IEEE Transactions on Geoscience and Remote Sensing, 43(10), 2177-2184.

Burkholder, R. J., Gupta, I. J., and J. T. Johnson, (2003), Comparison of Monostatic and Bistatic Radar Images, IEEE Antennas and Propagation Magazine, 45(3), 41-50.

Daout, F., Khenchaf, A., and J. Saillard, (1996), Calibration of bistatic polarimetric scatterometers, Geoscience and Remote Sensing Symposium, Lincoln, NE.

Eigel, R. L., Jr., Collins, P. J., Terzuoli, A. J., Nesti, G., and J. Fortuny, (2000), Bistatic scattering characterization of complex objects, IEEE Transactions on Geoscience and Remote Sensing, 38(5), 2078-2092.

Glaser, J. I., (1986), Fifty years of bistatic and multistatic radar, IEE Proceedings of Radar and Signal Processing, 133(7), 596-603.

Glaser, J. I., (1989), Some results in the bistatic radar cross section (RCS) of complex objects, Proceedings of the IEEE, 77(5), 639-648.

Griffiths, H., (2013), Bistatic and Multistatic Radar, IEEE AESS Distinguished Lecture, ETH Zurich.

Huang, Y., Yang J., and J. Xiong, (2006), Synchronization technology of bistatic radar system, International Conference on Communications, Circuits and Systems Proceedings, Guilin, China, 2219-2221.

Janse van Rensburg, D. J., and Pistorius, C. W. I., (1992), The compact antenna test range (CATR) at the University of Pretoria, 3rd AFRICON Conference, Ezulwini Valley, Swaziland, 175-177.

Kahny, D., Schmitt, K., and W. Wiesbeck, (1992), Calibration of bistatic polarimetric radar systems, IEEE Transactions on Geoscience and Remote Sensing, 30(5), 847-852.

Kesheng, L., (2003), An analysis of some problems of bistatic and multistatic radars, Proceedings of the International Radar Conference, Adelaide, Australia, 429-432.

Knott, E. F., Shaeffer, J., and M. Tuley, (2004), Radar Cross Section (RCS), USA: Scitech.

Monzon, C., (2003), A cross-polarized bistatic calibration device for RCS measurements," IEEE Transactions of Antennas and Propagation, 51(4), 833-839.

Pienaar, M., Odendaal, J. W., Cilliers, J. E., Smit, J. C., and J. Joubert, (2015), Dynamic Radar Calibrations with an Airborne Active Calibration Target, 1st URSI Atlantic Radio Science Conference (URSI AT-RASC 2015), Gran Canaria, Spain, 18-22.

Sarabandi, K., Ulaby, F. T., and M. A. Tassoudji, (1990), Calibration of Polarimetric Radar Systems with Good Polarization Isolation, IEEE Transactions on Geoscience and Remote Sensing, 28(1), 70-75.

Skolnik, M., (2008), Radar Handbook, 3rd edn. McGraw-Hill Professional, New York.

Vu, T. A., Dooghabadi, M. Z., Sudalaiyandi, S., Hjortland, H. A., Naess, O., Lande, T. S., and S. E. Hamran, (2009), UWB Vivaldi antenna for impulse radio beamforming, NORCHIP, Trondheim.